2020 17th International Conference on Electrical Engineering, Computing Science and Automatic Control (CCE)
Mexico City, Mexico. November 11-13, 2020

Properties Of Ultra-Thin Radio-frequency Sputtered Aluminum Doped Zinc Oxide Thin Films For Solar Cell Applications

Onyekachi Nwakanma
Department of Electrical Engineering (SEES), Centro de Investigación y de Estudios Avanzados del Instituto Politécnico Nacional (CINVESTAV-IPN), Mexico
onyekachi@cinvestav.mx

Velumani Subramaniam
Department of Electrical Engineering (SEES), Centro de Investigación y de Estudios Avanzados del Instituto Politécnico Nacional (CINVESTAV-IPN), Mexico
velu@cinvestav.mx

Arturo Morales-Acevedo
Department of Electrical Engineering (SEES), Centro de Investigación y de Estudios Avanzados del Instituto Politécnico Nacional (CINVESTAV-IPN), Mexico
amorales@solar.cinvestav.mx

***Abstract*— We optimized radio-frequency (RF) sputtering parameters for depositing low-thickness (ca 100 nm) aluminum-doped zinc oxide (AZO) for solar cell applications aimed at reducing optical losses commonly associated with transparent conducting oxides (TCO), which causes a significant reduction in the efficiency. X-ray diffraction (XRD) analysis and high-resolution scanning electron microscopy (HR-SEM) aided in studying the variations in the structure and morphology with deposition parameters and temperature. The optical characterizations using UV-Vis spectral measurements showed above 90% transmittance, with resistivity characterizations using four-point probe and Hall measurements. We defined a quality factor (QF) to characterize the performance of TCO layers, considering equally the resistivity and transmittance as they play vital roles in their TCO applications. The reported parameters produced films with lower resistivities and high QF for TCO applications with no use for post-deposition temperature treatments.**

Keywords*— quality factor (QF), aluminum-doped zinc oxide (AZO), rf sputtering, Transparent conducting oxide (TCO)

I. INTRODUCTION

The suitability for transparent conducting oxide (TCO) materials for photovoltaic applications depend on the bandgaps (~3.3 eV), high lateral conductance, and high carrier mobility, which allow for the transference of photo-generated current to the electrical contacts without significant losses [1,2].

The use of aluminum-doped zinc oxide (AZO) thin films as an alternative TCO layer to commonly used ITO depend on the comparable electrical and optical properties, with the choice of doping ZnO with aluminum among the other group III elements (Al, Ga, and In) primarily due to its low raw material cost [3–5]. The reported resistivity values of AZO films for TCO solar cell applications range between 1×10^{-4} to 10 Ω cm, and doping with Al (optimal between 1 and 3 at% [6]) modifies the defect density influencing the resistivity, optical, morphological, and lattice properties of the ZnO structure. The lower resistivity values attained with some post-deposition treatment, usually by annealing at elevated temperatures up to 500°C [6–8], may cause some detrimental effects during device fabrications (e.g., the diffusion of Al into the absorber layer) in the substrate configuration. The optimal deposition techniques and parameters [6,8–12] affect the properties of the deposited films, which in turn influences the efficiency of the solar cell device [13,14].

The regular use of radio-frequency (RF) deposition method as the preferred choice for AZO deposition is due to the potential for low-temperature growth, industrial applicability, relatively excellent uniformity, and reproducibility independent of deposition temperature [13,14].

Previous studies with thick AZO layers to reduce the resistivity of the layer show detrimental effects to the transmittance property of the layer. However, recent reports on high-efficiency solar cells show that low-thickness AZO layers can also provide excellent efficiency [12]. Furthermore, with recent studies aimed at developing ultra-thin devices [15–17], the deposition of ultra-thin AZO layers is of vital significance to the efficiency. Considering the resistivity and transmittance of the TCO layers, which possess equal importance for device fabrication, the evaluation of quantitative performance using a quality factor (QF) provides a tool for evaluating performance. We define the QF (similar to the figure of merit (FOM defined by [18]) as:

$$QF = \text{transmittance} \times \text{sheet conductance} = \text{transmittance/sheet resistance} \quad (1)$$

A sufficiently thin layer is required to achieve a high transmittance, which inversely causes a higher sheet resistance in the thin films. Thus, the above inverse relation puts a limit on the QF value.

This study aims at optimizing the RF sputtering parameters for depositing ultra-thin AZO films (~100 nm) with higher transmittance and comparatively low sheet resistances at moderate temperatures (< 200 °C) with no need further post-deposition treatment. We have no knowledge of any available prior literature on low thickness deposition of AZO at relatively low temperatures with the deposition parameters, as reported in this work.

II. EXPERIMENTS

A. Materials

The 10x10 cm^2 glass substrates (pre-cleaned plain Micro slides, Corning No 2947), Extran solution, sodium hydroxide pellets (NaOH, assay ≥ 98%), and hydrochloric acid (HCl) (ACS reagent, 37% assay) were all purchased from Sigma

978-1-7281-8987-1/20/$31.00 ©2020 IEEE

Aldrich and cleaned using the method described in [19]. We bought zinc oxide with Alumina target (ZnO/Al_2O_3, 98/2 wt%; 3.00" (76.2 mm) diameter and 0.250" (6.35 mm) thickness with 99.999% pure part) from Kurt J. Lesner. We purchase Argon (Ar, 99.99%) and nitrogen (N_2) gas cylinders from Infra group-Mexico (Industrial line standards).

B. Optimizing deposition parameters and results

The RF depositions with an operating frequency between 50-60 Hz, has the target-to-substrate distance was adjusted to about 6.0 cm and tilted to about 55° to the horizontal as these conditions affect physical deposition techniques [20]. The base pressure for all film depositions was approximately 5.0×10^{-6} Torr to avoid contamination from any residue gas in the sputtering chamber. Ambient depositions had the temperatures rise to ~43 ºC due to non-intentional heating. A substrate rotation of about 0.05 rpm was maintained in depositions to ensure the uniformity of the film over larger surface areas and reflected power of less than 3 W for all depositions.

The changes in sputtering power and pressure affect the kinetic energy and mean free path of the sputtered atomic species. Increasing the sputtering power at constant pressure increases the kinetic energy of the sputtering Ar ion, and thus the kinetic energy of the ejected ions, which results in increased deposition rates and thicker films. Alternatively, increasing the sputtering pressures causes reduced thickness due to increased collision of the sputtered atomic species and decreased mean free path.

The optimization results on thickness and resistivity characterizations for AZO films (Table I) deposited for 90 minutes at ambient temperatures showed variations with the working pressure and sputtering power. Increasing the sputtering power at a constant pressure value of 15 mTorr showed an accompanying reduction in resistivity and increased thickness.

The reduction in resistivity could be due to improved doping of the ZnO lattice with Al ions. Attempts at depositions with lower sputtering power (50 W or lesser) and higher pressure (≥15 mTorr) produces no measurable thickness and very high resistivity beyond the scale of our equipment. The poor deposition may be due to high entropy and less kinetic energy. We ignored a further increase in sputtering power (beyond 135 W) to accommodate the limits of the maximum power density of the target (20 W/inch^2).

At a constant sputtering power of 125 W, increasing the working pressure results in lesser thickness. We observed, however, that the resistivity of thin films tends to decrease with increasing pressure. Further increase in working pressure beyond 25 mTorr may present detrimental effects on the films, as evident on the very low deposition rates commonly associated with RF sputtering [14].

TABLE I. THICKNESS AND RESISTIVITY FOR VARYING SPUTTERING POWERS AND PRESSURES

Power (W)	Pressure (mTorr)	Average thickness (nm)	Resistivity (Ω cm)
50	15	--	--
75		70.8	8400
125		120.1	4.61
135		139.9	3.62
125	5	141.8	--
	15	120.1	4.61
	20	27.6	0.516
	25	14.4	0.304

Contrary to the observations during sputtering at lower pressures mainly for single elemental materials (e.g., Mo) [19,21,22], materials that require some doping tend to require some higher pressures to allow for incorporation of the dopant in the crystal structure.

C. Deposition at optimized power and temperature effects

Adopting an optimal sputtering power (125 W) and pressure (20 mTorr), we increased the deposition time (150 minutes) to improve on the thickness of the thin-film. The average thickness of the AZO thin films is 97 nm.

III. ANALYSIS OF RESULTS

A. Structural characterization

The X-ray diffractogram of the AZO films (Fig. 1) showed characteristic peaks of a hexagonal wurtzite structure (ICCD 00-036-1451), with preferred orientation and peak intensities varying with deposition parameters and temperature effects.

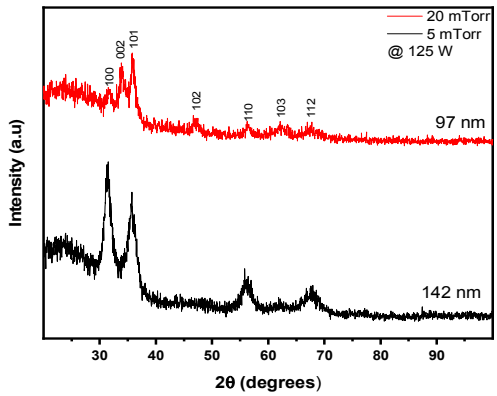

(a)

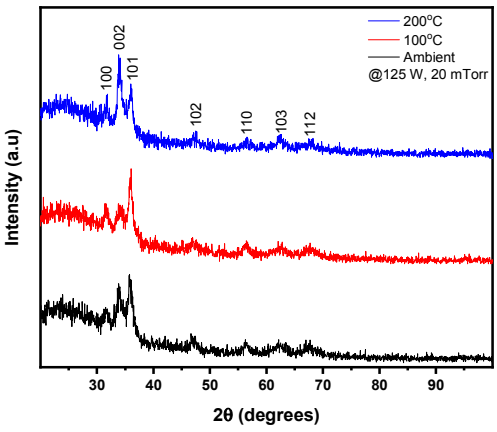

(b)

Fig. 1. XRD pattern of the AZO films deposited at (a) different pressures and the same power and (b) different temperatures

We observed the (002) peak position previously lacking in depositions with lower working pressure (5 mTorr) (Fig. 1a) as the pressure increased (20 mTorr), which could be due to the greater incorporation of Al within the crystal lattice. At a constant power of 125 W and 20 mTorr working pressure, the increase in substrate temperature (Fig. 1b) seemed to increase the relative peak intensity and induce a change in the preferred orientation from (101) to (002) at a substrate temperature of 200 oC, consistent with an increase in the atomic ratio of Al [8,11,23]. This inclusion of Al also reflects in the shift of the diffraction angle to a higher 2θ value and a marginal increase in the bond length, L (Table II).

TABLE II. LATTICE PARAMETERS OF AZO FILMS DEPOSITED AT 125 W AND 20 MTORR AT DIFFERENT TEMPERATURES: AMBIENT, 100°C AND 200°C

Temp. (°C)	**2θ (°)**	**FWHM (β)**	D **(nm)**	**a (Å)**	**c (Å)**	**c/a**	**L (Å)**
Ambient	35.76	0.472	18.5	3.253	5.295	1.628	1.990
100	35.93	0.630	13.8	3.273	5.270	1.610	1.995
200	36.12	0.394	36.7	3.261	5.305	1.627	1.994

B. Morphological analysis

The surface morphology of the AZO films (Fig. 2) showed the presence of randomly oriented grains, which appears to increase with the effects of temperature. The application of temperature gradient causes a reduction in the surface energy of ZnO [24] and allows for more incorporation of Al [25]. The increase in grain sizes offer better compactness and helps to decrease optical scattering [12].

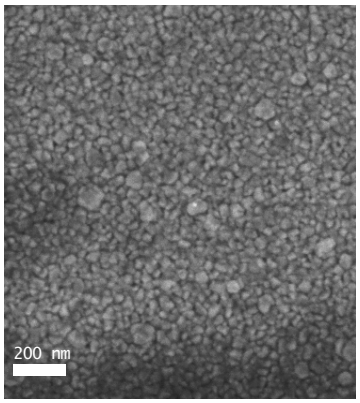

(a)

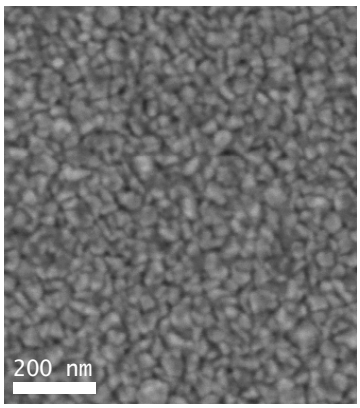

(b)

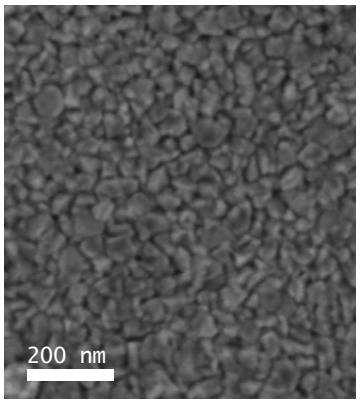

(c)

Fig. 2. Surface micrograph using FE-SEM for films deposited using 125 W and 20 mTorr at (a) ambient (b) 100 °C and (c) 200 °C

Elemental analysis for the percentage compositions in the AZO thin films using energy-dispersive spectroscopy (EDS) (Table III) shows that the composition of Al in the thin films increases with temperature.

TABLE III. ELEMENTAL COMPOSITION THE ELEMENTS FROM EDS ANALYSIS

	%Zn	**%Al**	**%O**	**Al/ (Al+Zn)**	**Zn/ (Al+Zn)**
Ambient	17.40	1.83	80.77	9.50	90.50
100 °C	16.05	1.89	82.06	10.5	89.5
200 °C	15.27	2.39	82.34	13.5	86.5

The increased Al content can also account for a potential increased conductivity of the films and a possible shift in the band-edge of the films.

C. Electrical measurements

The measured sheet resistance and calculated resistivity of the thin films decrease as the working pressure increases [26] at constant deposition power (Table IV). The decrease could be due to the higher inclusion of Al, causes the improvement in the electrical property and the changes in the structure and morphology of the thin film reported in the previous sections. The increase in resistivity as the pressure increases from 20 mTorr to 25 mTorr could be due to poor crystallization and very little thickness deposited.

TABLE IV. AVERAGE THICKNESS AND ELECTRICAL PARAMETERS FILMS DEPOSITED IN AMBIENT USING FOUR-POINT PROBE MEASUREMENT

Power (W)	**Pressure (mTorr)**	**Average thickness (nm)**	**Sheet Resistance (10^2 Ω/□)**	**Resistivity (10^{-3} Ω cm)**
125	5	367	569.6	2091
	10	246	6.412	15.75
	15	155	7.672	11.93
	20	97.9	4.276	4.186
	25	68.5	6.518	4.463

The characterization of thin films deposited at a constant power of 125 W and a pressure of 20 mTorr (Fig. 3) shows a variation in the resistivity values with the effects of temperature.

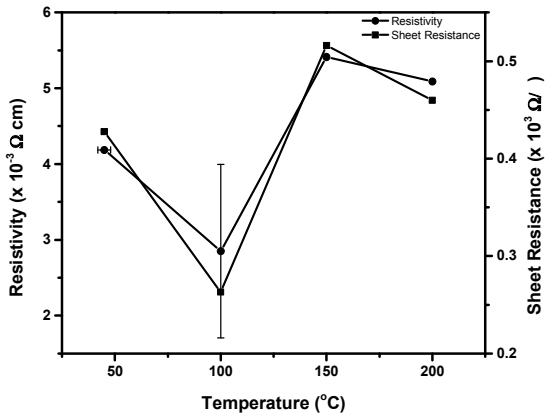

Fig. 3. Variation of sheet resistance (ρ_s) and resistivity (ρ) at different temperatures (with constant 125 W and 20 mTorr depositions)

With the application of temperature, we measured a decrease in sheet resistance and the calculated resistivity at from ambient to 100 oC depositions (Fig. 3). The increase in the resistivity at depositions with 200 oC substrate temperature could be due to a change in the crystal orientation and distortions in the lattice parameters with increased temperature [14].

D. Optical characterizations

The optical transmittance for TCO layers, desirable > 85 %, typically decreases with increasing thickness [27,28]. Since the resistivity of the thin films decreases with increasing thickness, there is a vital requirement to optimize the optical and electrical properties to minimize parasitic light absorption. The transmittance of the deposited AZO (Fig. 4) film showed relatively high values for all depositions. The deposition at a low pressure of 5 mTorr, which posses a higher thickness, as can be seen from the interference pattern, has a lower transmittance compared with the depositions with a lesser thickness (i.e., 20 mTorr).

The values of transmittance measured at 550 nm show that all the films deposited with the optimal condition (125 W and 20 mTorr), independent of the temperature, is above 90%.

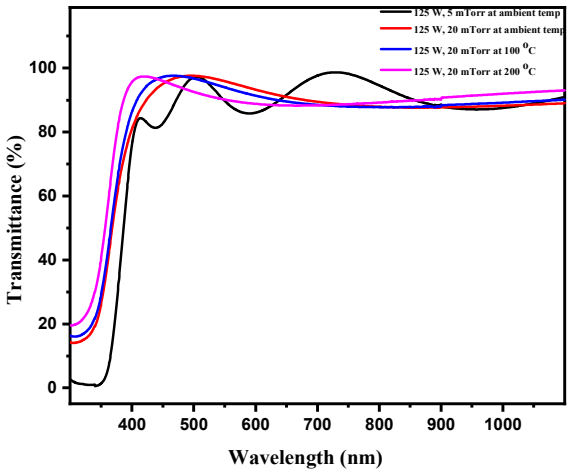

Fig. 4. The transmittance against wavelength for various AZO films (125 W, and varying pressures 5 to 20 mTorr) and varying temperatures

E. Quality factor (QF) calculation

The resistivity of a TCO is a relevant parameter, and the sheet resistance depends on the resistivity and thickness, which also affects the optical transmittance of each film. Therefore, all these parameters are interrelated. Then, there is a need to decide the best deposition conditions for the application of the TCO to solar cells. Using Eqn 1, the better conditions should be those who give the highest value of QF. Using the mentioned equation (1), we calculated the quality factor for the AZO films.

TABLE V. QF FOR THE FILMS DEPOSITED AT 125 W, 20 MTORR AT VARIOUS TEMPERATURES: AMBIENT, 100 °C AND 200 °C

Power (W)	Pressure (mTorr)	T (ºC)	%T	ρ_s (10^2 Ω/□)	ρ (10^{-3} Ω cm)	QF (10^{-3} Ω^{-1})
125	20	Ambient	95.92	4.276	4.186	2.243
		100	94.02	2.630	2.851	3.575
		200	90.18	4.598	5.090	1.961

Several indications, taking into account the measurements made, points to the best deposition temperature being 200 oC: table 1 showing larger crystallite size and reduced dislocation density, and larger grain sizes from the SEM micrographs. However, the QF mentioned above and (Table V) shows that the better condition for deposition is at 100 ºC, confirming that this is the best deposition temperature for solar cell applications.

IV. DISCUSSION OF THE SIGNIFICANCE OF THE WORK

The results in this study present an optimized sputtering condition for the fabrication of ultra-thin AZO layer (approx. 100 nm) thickness with high optical transmittance and excellent QF for TCO application. The proposed method is easily scalable for uniform film deposition and applicable to ultra-thin device fabrications.

V. SUMMARY

We successfully optimized conditions for low thickness AZO thin films with no further high-temperature post-deposition treatment, providing explanations to the changes observed with the application of substrate temperatures. Structural characterizations of films obtained with the optimized deposition conditions using XRD confirmed a successful deposition of hexagonal wurtzite structure, with bond length L of 1.995 Å, accounted for by the successful doping of ZnO lattice by Al ions. The morphological studies showed the effects of temperature in the grain sizes and distribution with EDS analysis showing the percentage inclusion of Al as the temperature is varied. With a high transmittance of 94% and resistivity of 2.851 x 10^{-3} Ω cm, the QF for the AZO films was 3.575 10^{-3} Ω^{-1}.

VI. ACKNOWLEDGMENT

We wish to acknowledge Consejo Nacional de Ciencia y Tecnología y la Secretaría de Energía (CONACyT-SENER) (Project 263043) and El Centro Mexicano de Innovación en Energía Solar (CEMIE-Sol P-55) for the financial support for this project. We also wish to acknowledge the following for their technical support, M. en C. Adolfo Tavira Fuentes (XRD measurements), and Ing. Miguel Ángel Luna Arias (thickness measurements), Norma Iris González García (contact depositions), Also, O.N thanks CONACyT for the doctoral scholarship.

REFERENCES

[1] G. Yin, A. Steigert, P. Manley, R. Klenk, M. Schmid, Enhanced absorption in tandem solar cells by applying hydrogenated In 2 O 3 as electrode, Appl. Phys. Lett. 107 (2015) 211901. https://doi.org/10.1063/1.4936328.

[2] K. Ellmer, A. Klein, B. Rech, eds., Transparent Conductive Zinc Oxide Basics and Applications in Thin Film Solar Cells, Springer Berlin Heidelberg, Berlin, Heidelberg, 2008. https://doi.org/10.1007/978-3-540-73612-7.

[3] A. Janotti, C.G. Van De Walle, Fundamentals of zinc oxide as a semiconductor, Reports Prog. Phys. 72 (2009). https://doi.org/10.1088/0034-4885/72/12/126501.

[4] K. Ellmer, Past achievements and future challenges in the development of optically transparent electrodes, Nat. Photonics. 6 (2012) 809–817. https://doi.org/10.1038/nphoton.2012.282.

[5] T. Minami, Transparent conducting oxide semiconductors for transparent electrodes, Semicond. Sci. Technol. 20 (2005) S35–S44. https://doi.org/10.1088/0268-1242/20/4/004.

[6] H. ming Zhou, D. qing Yi, Z. ming Yu, L. rong Xiao, J. Li, Preparation of aluminum doped zinc oxide films and the study of their microstructure, electrical and optical properties, Thin Solid Films. 515 (2007) 6909–6914. https://doi.org/10.1016/j.tsf.2007.01.041.

[7] T.R. Ramireddy, V. Venugopal, J.B. Bellam, A. Maldonado, J. Vega-Pérez, S. Velumani, MDLL Olvera, Effect of the milling time of the precursors on the physical properties of sprayed aluminum-doped zinc oxide (ZnO: Al) thin films, Materials (Basel). 5 (2012) 1404–1412. https://doi.org/10.3390/ma5081404.

[8] SO. El hamali, W.M. Cranton, N. Kalfagiannis, X. Hou, R. Ranson, D.C. Koutsogeorgis, Enhanced electrical and optical properties of room temperature deposited Aluminium doped Zinc Oxide (AZO) thin films by excimer laser annealing, Opt. Lasers Eng. 80 (2016) 45–51. https://doi.org/10.1016/j.optlaseng.2015.12.010.

[9] B.J. Babu, S. Velumani, J. Arenas-Alatorre, A. Kassiba, J. Chavez, H. Park, S.Q. Hussain, J. Yi, R. Asomoza, Structural Properties of Ultrasonically Sprayed Al-Doped ZnO (AZO) Thin Films: Effect of ZnO Buffer Layer on AZO, J. Electron. Mater. 44 (2014) 699–705. https://doi.org/10.1007/s11664-014-3541-3.

[10] S.J. Henley, M.N.R. Ashfold, D. Cherns, The growth of transparent conducting ZnO films by pulsed laser ablation, Surf. Coatings Technol. 177–178 (2004) 271–276. https://doi.org/10.1016/j.surfcoat.2003.09.005.

[11] T.M.K. Thandavan, S.M.A. Gani, C.S. Wong, R.M. Nor, Enhanced photoluminescence and Raman properties of Al-doped ZnO nanostructures prepared using thermal chemical vapor deposition of methanol assisted with heated brass, PLoS One. 10 (2015) 1–18. https://doi.org/10.1371/journal.pone.0121756.

[12] S. Paetel, Roadmap CIGS towards 25 % Efficiency, Zent. Für Sonnenenergie- Und Wasserstoff-Forsch. Baden-Württemb. (2016).

[13] K. S, J.J. Ríos-Ramírez, S. Chakaravarthy, V. S, Electrical, optical, and topographical properties of RF magnetron sputtered aluminum-doped zinc oxide (AZO) thin films complemented by first-principles calculations, J. Mater. Sci. Mater. Electron. 29 (2018) 15383–15395. https://doi.org/10.1007/s10854-018-8920-8.

[14] P.J.M. Isherwood, M. Gona, J.W. Bowers, N. Neves, P. Newbatt, J.M. Walls, Comparison of DC and RF sputtered aluminium-doped zinc oxide for photovoltaic applications, in: 2015 IEEE 42nd Photovolt. Spec. Conf., IEEE, 2015: pp. 1–5. https://doi.org/10.1109/PVSC.2015.7355900.

[15] G. Rajan, K. Aryal, S. Karki, P. Aryal, R.W. Collins, S. Marsillac, Characterization and Analysis of Ultrathin CIGS Films and Solar Cells Deposited by 3-Stage Process, J. Spectrosc. 2018 (2018) 1–9. https://doi.org/10.1155/2018/8527491.

[16] M. Boubakeur, A. Aissat, M. Ben Arbia, H. Maaref, J.P. Vilcot, Enhancement of the efficiency of ultra-thin CIGS/Si structure for solar cell applications, Superlattices Microstruct. 138 (2020) 106377. https://doi.org/10.1016/j.spmi.2019.106377.

[17] G. Yin, V. Brackmann, V. Hoffmann, M. Schmid, Enhanced performance of ultra-thin Cu(In,Ga)Se2 solar cells deposited at low process temperature, Sol. Energy Mater. Sol. Cells. 132 (2015) 142–147. https://doi.org/10.1016/j.solmat.2014.08.045.

[18] G. Haacke, New figure of merit for transparent conductors, J. Appl. Phys. 47 (1976) 4086–4089. https://doi.org/10.1063/1.323240.

[19] O. Nwakanma, P. Reyes, S. Velumani, Electrical, structural, and topographical properties of direct current (DC) sputtered bilayer molybdenum thin films, J. Mater. Sci. Mater. Electron. 29 (2018) 15671–15681. https://doi.org/10.1007/s10854-018-9165-2.

[20] D.M. Mattox, Handbook of Physical Vapor Deposition (PVD) Processing, in: Handb. Phys. Vap. Depos. Process., Elsevier, 1998: p. 746. https://doi.org/10.1016/B978-081551422-0.50001-2.

[21] A. Morán, O. Nwakanma, S. Velumani, H. Castaneda, Comparative study of optimised molybdenum back-contact deposition with different barriers (Ti, ZnO) on stainless steel substrate for flexible solar cell application, J. Mater. Sci. Mater. Electron. 31 (2020) 7524–7538. https://doi.org/10.1007/s10854-020-03058-7.

[22] J.H. Scofield, A. Duda, D. Albin, B.L. Ballard, P.K. Predecki, Sputtered molybdenum bilayer back contact for copper indium diselenide-based polycrystalline thin-film solar cells, Thin Solid Films. 260 (1995) 26–31. https://doi.org/10.1016/0040-6090(94)06462-8.

[23] C. Jeong, H.S. Kim, D.R. Chang, K. Kamisako, Effect on Al 2 O 3 doping concentration of RF magnetronl sputtered ZnO:Al films for solar cell applications, Jpn. J. Appl. Phys. 47 (2008) 5656–5658. https://doi.org/10.1143/JJAP.47.5656.

[24] D. Raoufi, Synthesis and photoluminescence characterization of ZnO nanoparticles, J. Lumin. (2013). https://doi.org/10.1016/j.jlumin.2012.08.045.

[25] Y. Kajikawa, Texture development of non-epitaxial polycrystalline ZnO films, J. Cryst. Growth. (2006). https://doi.org/10.1016/j.jcrysgro.2005.11.089.

[26] MA Green, Solar cells—Operating principles, technology and system applications, Sol. Energy. 28 (1982) 447. https://doi.org/10.1016/0038-092X(82)90265-1.

[27] Z. Chen, W. Li, R. Li, Y. Zhang, G. Xu, H. Cheng, Fabrication of highly transparent and conductive indium-tin oxide thin films with a high figure of merit via solution processing, Langmuir. 29 (2013) 13836–13842. https://doi.org/10.1021/la4033282.

[28] U. Betz, M. Kharrazi Olsson, J. Marthy, M.F. Escolá, F. Atamny, Thin films engineering of indium tin oxide: Large area flat panel displays application, Surf. Coatings Technol. 200 (2006) 5751–5759. https://doi.org/10.1016/j.surfcoat.2005.08.144.